Continence 18 (2026) 102332

Contents lists available at ScienceDirect

Continence

journal homepage: www.elsevier.com/locate/cont

Regional differences in sensory afferent innervation of the mouse bladder wall

Susana Fernández Chadily [a], Marianne E. van Klaveren [a], Melissa Schepers [c,d], Tim Vanmierlo [c,d], John Heesakkers [a,b], Lori A. Birder [e], Gommert A. van Koeveringe [a,b], Mathijs M. de Rijk [a,b,*]

[a] Department of Urology, Mental Health and Neuroscience Research Institute, Faculty of Health, Medicine and Life Sciences, Maastricht University, Maastricht, the Netherlands
[b] Department of Urology, Maastricht University Medical Center+ (MUMC+), Maastricht, the Netherlands
[c] Department Psychiatry and Neuropsychology, Mental Health and Neuroscience Research Institute, Maastricht University, Maastricht, the Netherlands
[d] Department of Neuroscience, BIOMED, Hasselt University, Diepenbeek, Belgium
[e] Department of Medicine, University of Pittsburgh School of Medicine, Pittsburgh, PA, USA

ARTICLE INFO

Keywords:
Lower urinary tract
Calcitonin gene–related peptide
Afferent fibers
Immunohistochemistry
Mouse bladder

ABSTRACT

Background and objective: Sensory afferent innervation of the bladder wall is critical for regulating lower urinary tract function. Calcitonin gene–related peptide (CGRP) is a neuropeptide expressed predominantly in unmyelinated C-fibers and serves as a marker of sensory afferent fibers. While previous studies suggested regional differences in bladder innervation, quantitative evidence across the rostro–caudal axis is lacking. Here, we systematically quantified regional differences in CGRP-positive afferent innervation across the mouse bladder.
Methods: Bladder tissue from nine mice was processed and stained for CGRP immunofluorescence. Images were segmented into seven equal rostro–caudal regions from bladder dome to bladder neck, and CGRP-positive area was quantified and normalized to total tissue area. A permutation testing approach was applied to determine whether CGRP increased along the rostro–caudal axis.
Key findings and limitations: CGRP-positive fibers were detected throughout the bladder wall and showed a gradual increase in CGRP-positive area from dome to bladder neck. Linear regression analysis across segment means yielded a positive slope ($\beta = 0.0095$). Exact permutation testing across all 5040 possible segment arrangements showed that only 1.7% of permuted datasets produced slopes equal to or greater than the observed value ($p = 0.0171$). These results confirm that CGRP-positive afferent innervation of the mouse bladder wall is not evenly distributed but follows an exponential-like gradient along the rostro–caudal axis, with higher density toward the bladder neck.
Conclusions: These findings establish a quantitative baseline for regional sensory organization and may inform studies of pathological remodeling and new region-targeted therapies.

1. Introduction

The bladder, together with the urethra and urethral sphincter complex, form the lower urinary tract (LUT), which plays a critical role in maintaining homeostasis by storing and eliminating urine. This process relies on precise sensory signaling between the bladder and the central nervous system (CNS) [1]. Sensory afferent fibers located in the bladder wall consist mainly of two types: small myelinated Aδ-fibers and unmyelinated C-fibers. Aδ-fibers are primarily responsible for conveying mechanosensory information under physiological filling conditions, providing the CNS with essential input required to initiate and coordinate normal micturition [2]. By contrast, unmyelinated C-fibers are usually silent in healthy states but become active during inflammation, exposure to noxious chemical stimuli in the urine, or abnormal

* Corresponding author. Department of Urology, Mental Health and Neuroscience Research Institute, Faculty of Health, Medicine, and Life Sciences, Maastricht University, Universiteitssingel 40, Maastricht, 6229 ER, the Netherlands.
E-mail addresses: susana.chadily@maastrichtuniversity.nl (S. Fernández Chadily), a.vanklaveren@student.maastrichtuniversity.nl (M.E. van Klaveren), m.schepers@maastrichtuniversity.nl (M. Schepers), t.vanmierlo@maastrichtuniversity.nl (T. Vanmierlo), john.heesakkers@mumc.nl (J. Heesakkers), lbirder@pitt.edu (L.A. Birder), g.van.koeveringe@mumc.nl (G.A. van Koeveringe), m.derijk@maastrichtuniversity.nl (M.M. de Rijk).

https://doi.org/10.1016/j.cont.2026.102332
Received 31 January 2026; Received in revised form 23 March 2026; Accepted 23 March 2026
Available online 24 March 2026

overdistension. When activated, C-fibers transmit nociceptive, chemosensitive, and thermal signals to the CNS [1]. Within the bladder, calcitonin gene–related peptide (CGRP) is a neuropeptide expressed predominantly in unmyelinated C-fibers and, to a lesser extent, in small myelinated Aδ-fibers [3]. Through these afferent pathways, CGRP contributes to the transmission of bladder sensory information. Disruptions or maladaptation in this sensory communication have been associated with a range of LUT dysfunctions, including overactive bladder (OAB), urgency urinary incontinence, and bladder pain [4–6]. In OAB, hypersensitivity of afferent pathways is thought to drive the hallmark symptoms of urgency and frequency [6,7]. Likewise, bladder pain syndromes, including interstitial cystitis, have been linked to altered afferent signaling, where excessive or dysfunctional input from nociceptive fibers contributes to pain perception [8]. Experimental studies further support a role for sensory afferents in bladder dysfunction. CGRP is up-regulated in animal models of bladder pain and inflammation, suggesting increased excitability or plasticity of these fibers under pathological conditions [9]. Reviews of neuropeptide signaling in bladder pain syndromes also highlight the contribution of CGRP and other sensory mediators, reinforcing the notion that disturbances in sensory neurotransmission are central to LUT dysfunction [5].

The bladder wall consists of several layers that contribute to its sensory and mechanical functions. The innermost lining is the urothelium, which acts not only as a permeability barrier but also as a sensory structure capable of releasing signaling molecules, such as ATP, acetylcholine, and prostaglandins, in response to stretch or chemical stimulation [2]. Immediately beneath lies the lamina propria, a connective tissue layer that contains a dense network of blood vessels, interstitial cells, and sensory nerve fibers, positioning it as a key location for afferent signaling [10]. These afferent fibers run close to the urothelium to detect bladder distension as well as chemical mediators released from urothelial cells [2]. Together, the urothelium and lamina propria form the mucosa, which is increasingly recognized as the functional center of the bladder wall [2,10]. The detrusor muscle and the serosa constitute the other major layers of the bladder wall. Regionally, the bladder can be divided along its rostro-caudal axis, with the dome (rostral region) at the top and the trigone (caudal region, between the ureteral orifices and urethra) at the base. In addition, differences in innervation have also been reported between the anterior and posterior bladder wall (fundus), suggesting that regional specialization is not limited to the dome–trigone axis [11]. While sensory afferent nerve fibers are present throughout the urothelium and lamina propria, the trigone has been recognized as a sensory hub with higher density of afferent nerve fibers compared to other regions [12]. In rats, for example, it has been suggested that CGRP-immunoreactive axons are more abundant in the bladder base and trigone compared to the dome, where the subepithelial plexus appears progressively sparser [11]. Consistent with these results, computer-assisted three-dimensional nerve tracking in the mouse bladder lamina propria showed greater nerve segment length in the trigone compared to the dome, suggesting structural specialization in the caudal bladder wall [13].

Despite these insights, many studies focused only on restricted areas (e.g., trigone vs dome) rather than mapping the full rostro-caudal axis and relied on semi-quantitative approaches. Moreover, little is known about the baseline regional distribution of sensory afferents in young, healthy animals, which is essential for interpreting age-related or pathological changes. A recent study investigated bladder sensory innervation in the context of aging, showing that the trigone of aged rats contains significantly less CGRP-positive area compared to young controls, suggesting that loss of sensory input may contribute to impaired LUT function with age [14]. While previous studies suggest that LUT-associated conditions can alter bladder afferent innervation, it remains unclear whether such changes affect all regions of the bladder equally or follow region-specific patterns. Addressing this question requires first establishing a systematic baseline of sensory innervation across the different functional regions of the healthy bladder.

In the present study, we aimed to systematically quantify regional differences in CGRP-positive sensory afferent innervation across the mouse bladder. Using immunohistochemistry for CGRP, combined with image analysis, we assessed whether innervation density varies along the rostro-caudal axis. We hypothesized that CGRP-positive sensory fibers are not evenly distributed across the bladder wall but instead follow a gradient, with higher density in caudal regions (towards the bladder neck) compared to rostral regions (dome).

2. Materials & methods

2.1. Tissue collection and preparation

Bladder tissues were collected as surplus post-mortem material from 10-week-old female C57BL/6J OlaHsd mice (Envigo, The Netherlands). The animals were maintained in a controlled temperature environment (21–22 °C) with a normal day-night rhythm (lights on 07:00am, lights off 07:00pm), with ad libitum access to food and water. Soft background noise was provided by a radio playing continuously in the housing room. All procedures were carried out in accordance with EU Directive 2010/63/EU on the protection of animals used for scientific purposes. No additional animals were sacrificed, and no animal procedures were performed specifically for the purpose of the present study. Mice were sacrificed by transcardial perfusion (PBS/heparin) after a lethal 200 mg/kg dolethal injection. Bladders were collected (N = 9), opened longitudinally and pinned flat with the lumen side upwards. Tissue was immediately immersion-fixed in 4% paraformaldehyde (PFA) in phosphate-buffered saline (PBS) for 60 min at room temperature (RT) to preserve tissue morphology and antigenicity. After fixation, samples were cryoprotected in 30% sucrose in PBS until fully infiltrated for >24 h, embedded in optimal cutting temperature (OCT) compound (Tissue-Tek, Sakura Finetek), and stored at −80 °C until further use. Tissue was serially sectioned at 20 µm on a cryostat and mounted on Superfrost Plus slides (Thermo Fisher Scientific) with 3 sections per slide, and 3 slides per animal.

2.2. Immunohistochemistry

Immunofluorescence staining was performed using a two-day protocol to detect CGRP, an established marker of sensory afferent fibers. Sections were washed in Tris-buffered saline (TBS) and encircled with a hydrophobic barrier (PAP pen). Non-specific binding was blocked with 1% normal donkey serum (NDS) dissolved in 0.3% Triton X-100 in TBS (TBS-T) for 1 h at RT. Sections were then incubated overnight at RT with a goat polyclonal primary antibody against CGRP (Abcam, ab36001; dilution 1:200 in TBS-T + 0.1% NDS). The antibody used in this study (Abcam, ab36001) is validated by the manufacturer for immunohistochemistry in mouse and rat tissues and has been widely used in rodent studies. Negative control sections were processed in parallel without primary antibody. Slides were then washed sequentially in TBS-T and TBS, followed by incubation with Alexa Fluor 647-conjugated donkey anti-goat secondary antibody (1:200, Thermo Fisher Scientific) for 1.5 h at RT. Nuclei were counterstained with Hoechst 33342 (1:1000 in TBS, 5 min). After final washes in TBS, slides were mounted with 80% glycerol in PBS to preserve fluorescence.

Fluorescent images were acquired using µManager software ver2.0 with identical exposure settings across samples on an Olympus BX51WI spinning-disk confocal fluorescence microscope with a Hamamatsu EM-CCD C9100 digital camera equipped with appropriate filter sets for Alexa Fluor 647 and DAPI. Images were saved in TIFF format for subsequent processing.

Image analysis was performed using ImageJ (Fiji, version 1.54p). A custom macro was developed to automate analysis steps, including [1]: channel separation and selection of the CGRP channel [2]; uniform background subtraction (radius = 50 pixels) applied to all images [3]; application of a fixed pixel intensity threshold range (lower = 1750,

upper = 6500) to the CGRP channel to generate a binary mask of the CGRP-positive signal [4]; segmentation of each image into seven equal-length regions along the rostro-caudal axis (dome to bladder neck); and [5] quantification of CGRP-positive area as percentage of total tissue area per segment. The segmentation approach allowed systematic comparison of CGRP signal along the full bladder strip from the dome to the bladder neck, and the normalization was done to correct for variability in tissue distribution across regions. Each CGRP-positive area of 10 or more connected pixels was included.

2.3. Statistical analysis

To assess whether CGRP expression followed a systematic rostro-caudal gradient, we used a permutation testing approach. For each animal, the CGRP-positive area was quantified across seven equal-length bladder segments. Nine sections per animal were analyzed. To reduce the influence of local outliers and section-to-section variability within animals, CGRP-positive area was summarized per segment using the median across images for each animal. These per-animal median values were subsequently used to calculate group-level mean ± SD values. A linear regression model was then fitted with segment position as the independent variable and CGRP-positive area as the dependent variable, yielding an observed slope (β).

To establish the null distribution, segment labels were permuted across all possible arrangements of the seven segments, which amounts to 5040 unique permutations (7! = 5040 permutations). For each permutation, a regression slope was recalculated, resulting in a distribution of slopes expected under the null hypothesis of no rostro-caudal organization. The empirical *p*-value was computed as the proportion of permuted slopes equal to or greater than the observed slope. All analyses were performed in MATLAB R2023b (MathWorks, Natick, MA), and visualization of the null distribution was generated using built-in plotting functions. A significant threshold of $p < 0.05$ was applied.

3. Results

To assess whether CGRP-positive afferent innervation exhibits a systematic gradient along the rostro-caudal axis of the mouse bladder, we quantified CGRP-positive area across seven equal-length segments from nine young mice. Negative control sections, processed in parallel without primary antibody, showed only background autofluorescence, confirming the absence of non-specific binding. Representative images illustrating CGRP expression in young bladder tissue are shown in Fig. 1. The CGRP-positive structures appear as elongated filamentous profiles consistent with sensory nerve fibers. For each segment, the median CGRP-positive area was first calculated per animal (9 images per segment per animal; 81 images total across all animals), after which segment-wise mean ± SD values were obtained across animals. Fig. 2 displays these normalized CGRP-positive area across segments. We then computed the slope of a linear regression across segment means. The observed slope was positive (β = 0.0095), indicating an increase in CGRP signal toward the caudal regions.

To evaluate the statistical significance of this rostro–caudal pattern, we performed an exact permutation test. This generated a null distribution of slopes centered around zero, against which the observed slope was compared (Fig. 3). The observed slope (0.0095, red dashed line) lay in the extreme right tail of the distribution, with only 1.7% of permuted datasets producing values equal to or greater, corresponding to a significance level of $p = 0.0171$. These results demonstrate that the increase in CGRP expression along the rostro-caudal axis is unlikely to be due to random variation and instead reflects a systematic gradient increase in bladder sensory innervation.

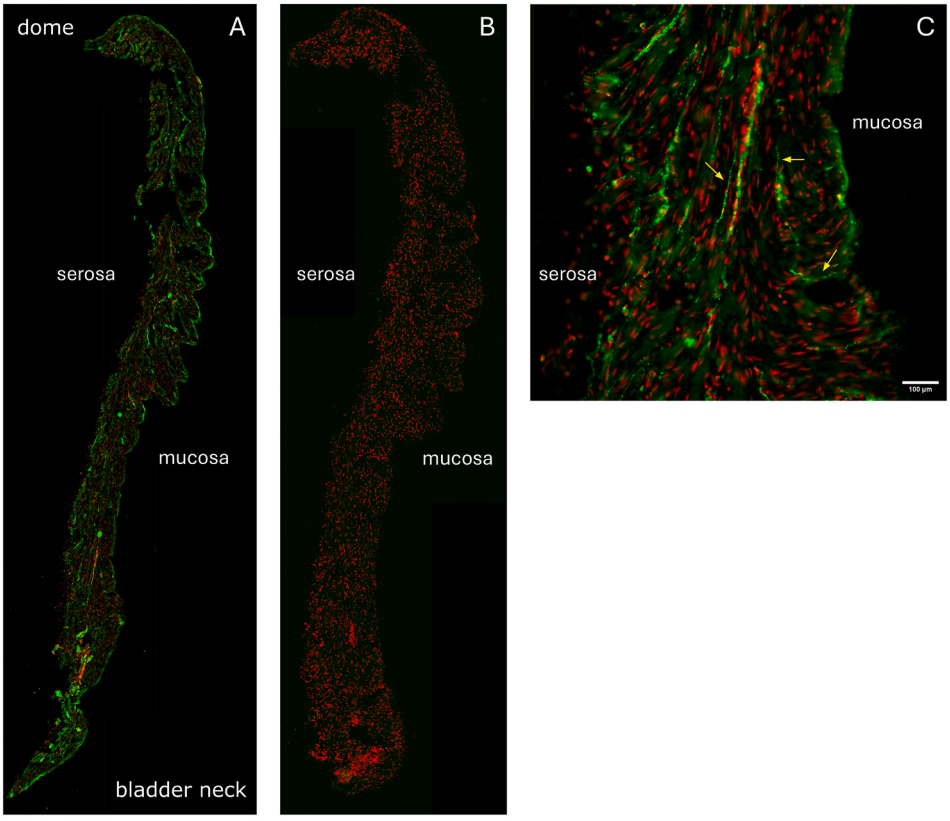

Fig. 1. A) Representative longitudinal section of mouse bladder spanning from the dome (rostral) to the bladder neck (caudal), illustrating the rostro–caudal orientation of the tissue. (B) Negative control section processed without primary antibody, showing only minor background autofluorescence and neuclei in red. (C) Higher-magnification image showing CGRP-positive sensory fibers within the bladder wall (arrows). CGRP immunofluorescence is shown in green and DAPI nuclear staining is shown in red. Scale bar = 100 µm.

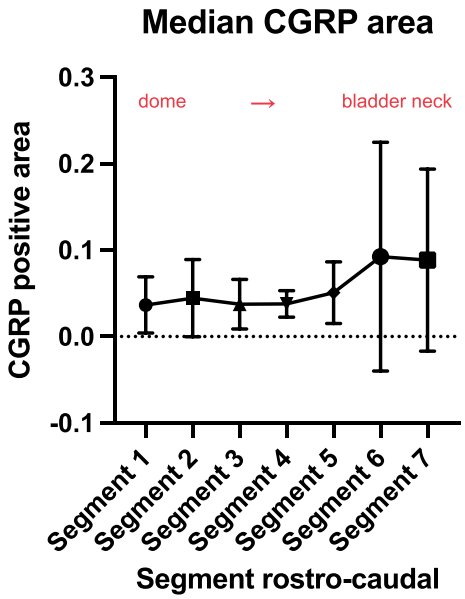

Fig. 2. Average and standard deviation of median CGRP-positive area normalized to detected tissue area across 7 rostro-caudal bladder segments, from the bladder dome to the bladder neck (N = 9).

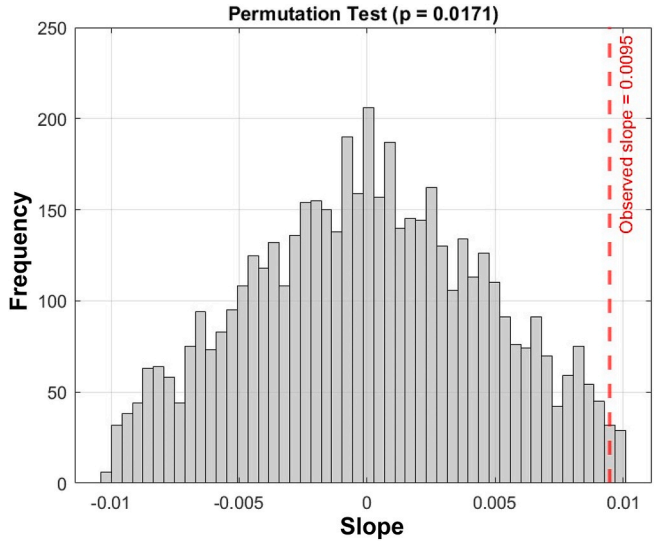

Fig. 3. Permutation test for the slope of CGRP-positive area across bladder segments. The histogram shows the null distribution of slopes obtained by randomly shuffling segment order (7! = 5040 permutations). The observed slope (0.0095, red dashed line) lies in the extreme right tail of the distribution, with only 1.7% of permuted datasets producing an equal or greater value (p = 0.0171).

4. Discussion

In the current study, we provide quantitative evidence that CGRP-positive sensory afferent innervation is not evenly distributed across the mouse bladder wall but instead follows a gradual rostro–caudal increase, with higher density toward the caudal regions, including the bladder neck. Previous studies had qualitatively suggested that the trigone accommodates a denser innervation compared to the dome or anterior wall [11–13], but to our knowledge, this is the first quantitative demonstration of such a gradient across the full rostro–caudal axis in young, healthy mice. Establishing a quantitative baseline of regional sensory organization in the healthy bladder is essential for interpreting region-specific changes in models of aging, inflammation, or bladder dysfunction.

The finding presented in the current study is consistent with the caudal aspect of the bladder, most importantly the trigone, being recognized as a sensory hub. Anatomical and functional studies have shown that afferent fibers, particularly unmyelinated C-fibers, are enriched in the trigone and closely associated with the urothelium and lamina propria, positioning this region for rapid sensory signaling [11, 12]. Our quantitative approach supports and extends these observations by confirming a graded increase in CGRP expression from dome to bladder neck. Although the overall magnitude of this gradient is modest, it is consistent with previous reports of increased sensory innervation in caudal bladder regions.

Such regional specialization is likely to have functional significance. The trigone plays a critical role in sensing flow-related stimuli and is highly responsive to chemical and mechanical stimulation [1,2]. Higher CGRP-positive afferent density in this region may reflect enhanced capacity to detect chemical irritation or noxious stimuli. Conversely, disruption or loss of this dense afferent network may disproportionately impair LUT function, as has been observed in aging [14].

Altered afferent signaling is a hallmark of multiple bladder disorders. In OAB, hypersensitivity of Aδ- and C-fiber pathways is thought to underlie urgency and frequency [6,7]. In bladder pain syndrome/interstitial cystitis, excessive nociceptive input from C-fibers contributes to pain [8,9]. Importantly, these disorders may not affect the bladder uniformly and therefore may require region-specific therapeutic targeting. As suggested by aging studies in rodents, there may be selective reductions in trigonal CGRP-positive fibers compared to the dome [14]. This observation raises the possibility that afferent loss follows a region-specific pattern. Similarly, in inflammation models, CGRP expression is upregulated in bladder afferents [9], but whether this occurs uniformly across the bladder wall is unknown. Our data emphasizes the importance of considering regional specificity when evaluating afferent remodeling in disease models, and we propose an approach to quantify these differences along the rostro-caudal axis.

Understanding the regional distribution of bladder afferents has direct therapeutic implications. For example, botulinum toxin A (BoNT-A), a widely used treatment for OAB and interstitial cystitis, not only reduces detrusor muscle contractility by blocking acetylcholine release at the neuromuscular junction but also exerts significant effects on sensory pathways. Several studies have shown that BoNT-A decreases the expression of sensory receptors in suburothelial afferents and suppresses urothelial release of neurotransmitters such as ATP, thereby reducing the excitability of C-fibers [15–17]. Targeting regions with dense afferent innervation, such as the trigone, may therefore enhance therapeutic outcomes, consistent with reports suggesting improved efficacy of trigone-specific injection protocols [18,19]. Beyond BoNT-A, future interventions aimed at modulating sensory activity may be optimized by incorporating knowledge of regional afferent organization. Achieving this, however, will depend on identifying molecular features that enable selective mechanism of action within the trigone. Considering the translational relevance of the findings presented here, it is important to note that regional afferent organization likely differs across species. The extent to which similar rostro–caudal gradients exist in the human bladder and whether disease might alter neural distribution in human tissue remains unclear.

In addition to these interpretative considerations, several methodological limitations should be acknowledged. First, although the bladders were cut longitudinally and pinned without applying tension, the exact location of each incision (anterior, posterior, or lateral wall) could not be determined. As a result, the precise position of the imaged tissue within each bladder strip remains unknown. Second, although the bladder was pinned open symmetrically, with the bladder neck positioned at the center of the caudal end of the strip, this process inevitably alters its native geometry. This, in turn, affects the relative rostro-caudal contributions to each equal-length segment and may explain the higher

variability observed in distal segments. Although the approach yields reproducible rostro-caudal quantification, interpretation must account for these geometric constraints, including the possibility that the trigone may be absent in a given strip due to uncontrolled incision orientation.

Future studies should address these limitations by standardizing the incision location to ensure that the trigone is consistently represented in the imaged bladder strips. Additionally, they should extend this quantitative approach to models of aging, inflammation, and OAB to determine whether the rostro–caudal gradient is preserved, diminished, or reversed under pathological conditions. In addition, while CGRP is a robust marker for C-fibers and a subset of Aδ-fibers, it does not capture the entire spectrum of afferent subtypes. In addition, modern approaches such as single-cell or single-nucleus sequencing of dorsal root ganglia, as well as spatial transcriptomics, may help further resolve the molecular diversity of bladder-innervating sensory neurons and their regional organization. Complementary markers or functional assays will be needed to fully characterize the diversity of sensory innervation across bladder regions, particularly to map fibers involved in processing bladder fullness. Finally, our analysis focused on the rostro–caudal axis; lateral differences (anterior vs posterior wall) may also be relevant and warrant further investigation.

In conclusion, our findings demonstrate that sensory innervation of the bladder wall is not homogeneously distributed but instead follows a gradual increase along the rostro-caudal axis. These results establish a quantitative baseline for regional afferent organization in the healthy mouse bladder and provide a framework for studying how disease and aging remodel sensory inputs. By revealing systematic regional differences, this work also highlights the potential for targeted therapeutic strategies that account for spatial heterogeneity in bladder innervation and to advance our understanding of spatial functional organization of different components of the LUT.

CRediT authorship contribution statement

Susana Fernández Chadily: Writing – review & editing, Writing – original draft, Visualization, Methodology, Investigation, Formal analysis, Data curation. **Marianne E. van Klaveren:** Writing – review & editing, Investigation, Formal analysis, Data curation. **Melissa Schepers:** Writing – review & editing, Methodology, Investigation, Data curation. **Tim Vanmierlo:** Writing – review & editing, Resources. **John Heesakkers:** Writing – review & editing, Resources. **Lori A. Birder:** Writing – review & editing, Conceptualization. **Gommert A. van Koeveringe:** Writing – review & editing, Resources, Methodology, Conceptualization. **Mathijs M. de Rijk:** Writing – review & editing, Writing – original draft, Visualization, Supervision, Resources, Methodology, Investigation, Formal analysis, Data curation, Conceptualization.

Funding

This research did not receive any specific grant from funding agencies in the public, commercial, or not-for-profit sectors.

Ethics approval

The authors declare that this study involves Animals but ethics approval is not needed for the following reason: Bladder tissues were collected as surplus post-mortem material from 10-week-old female C57BL/6J OlaHsd mice (Envigo, The Netherlands). All procedures were carried out in accordance with EU Directive 2010/63/EU on the protection of animals used for scientific purposes. No additional animals were sacrificed, and no animal procedures were performed specifically for the purpose of the present study.

Declaration of generative AI in scientific writing

During the preparation of this work, the authors used ChatGPT (OpenAI) to improve grammar, clarity, and overall language quality. After using this tool, the authors reviewed and edited the content as needed and take full responsibility for the content of the publication.

Declaration of competing interest

None of the authors report any potential conflict of interest relevant to this article.

Data availability

The datasets generated and analyzed during the current study, as well as the supporting analytical code, are available from the corresponding author upon reasonable request.

References

[1] W.C. de Groat, N. Yoshimura, Afferent nerve regulation of bladder function in health and disease, Handb. Exp. Pharmacol. (194) (2009) 91–138, https://doi.org/10.1007/978-3-540-79090-7_4. PubMed PMID: 19655106; PubMed Central PMCID: PMC3383010.

[2] L. Birder, K.E. Andersson, Urothelial signaling, Physiol. Rev. 93 (2) (2013) 653–680, https://doi.org/10.1152/physrev.00030.2012. PubMed PMID: 23589830; PubMed Central PMCID: PMC3768101.

[3] P.W. McCarthy, S.N. Lawson, Cell type and conduction velocity of rat primary sensory neurons with calcitonin gene-related peptide-like immunoreactivity, Neuroscience 34 (3) (1990) 623–632, https://doi.org/10.1016/0306-4522(90)90169-5. PubMed PMID: 2352644.

[4] A.M. Suskind, The aging overactive bladder: a review of aging-related changes from the brain to the bladder, Curr Bladder Dysfunct Rep 12 (1) (2017) 42–47, https://doi.org/10.1007/s11884-017-0406-7. PubMed PMID: 28947924; PubMed Central PMCID: PMC5609730.

[5] M. Wyndaele, A. Charrua, F. Herve, P. Aronsson, L. Grundy, V. Khullar, et al., Beyond the urothelium: interplay between autonomic nervous system and bladder inflammation in urinary tract infection, bladder pain syndrome with interstitial cystitis and neurogenic lower urinary tract dysfunction in spinal cord injury-ICI-RS 2023, Neurourol. Urodyn. 43 (6) (2024) 1283–1292, https://doi.org/10.1002/nau.25310. PubMed PMID: 37876314.

[6] W.D. Steers, Pathophysiology of overactive bladder and urge urinary incontinence, Rev. Urol. 4 (Suppl 4) (2002) S7–S18. PubMed PMID: 16986023; PubMed Central PMCID: PMC1476015.

[7] L. Grundy, A. Caldwell, S.M. Brierley, Mechanisms underlying overactive bladder and interstitial cystitis/painful bladder syndrome, Front. Neurosci. 12 (2018) 931, https://doi.org/10.3389/fnins.2018.00931. PubMed PMID: 30618560; PubMed Central PMCID: PMC6299241.

[8] N. Yoshimura, T. Oguchi, H. Yokoyama, Y. Funahashi, S. Yoshikawa, Y. Sugino, et al., Bladder afferent hyperexcitability in bladder pain syndrome/interstitial cystitis, Int. J. Urol. 21 (1) (2014) 18–25, https://doi.org/10.1111/iju.12308. PubMed PMID: 24807488; PubMed Central PMCID: PMC4089034.

[9] L.Y. Qiao, J.R. Grider, Up-regulation of calcitonin gene-related peptide and receptor tyrosine kinase TrkB in rat bladder afferent neurons following TNBS colitis, Exp. Neurol. 204 (2) (2007) 667–679, https://doi.org/10.1016/j.expneurol.2006.12.024. PubMed PMID: 17303123; PubMed Central PMCID: PMC1906719.

[10] K.E. Andersson, K.D. McCloskey, Lamina propria: the functional center of the bladder? Neurourol. Urodyn. 33 (1) (2014) 9–16, https://doi.org/10.1002/nau.22465. PubMed PMID: 23847015.

[11] G. Gabella, C. Davis, Distribution of afferent axons in the bladder of rats, J. Neurocytol. 27 (3) (1998) 141–155, https://doi.org/10.1023/a:1006903507321. PubMed PMID: 10640174.

[12] J.T. Purves, L. Spruill, E. Rovner, E. Borisko, A. McCants, E. Mugo, et al., A three dimensional nerve map of human bladder trigone, Neurourol. Urodyn. 36 (4) (2017) 1015–1019, https://doi.org/10.1002/nau.23049. PubMed PMID: 27265789.

[13] A. Schueth, B. Spronck, M. van Zandvoort, G.A. van Koeveringe, Computer-assisted three-dimensional tracking of sensory innervation in the murine bladder mucosa with two-photon microscopy, J. Chem. Neuroanat. 85 (2017) 43–49, https://doi.org/10.1016/j.jchemneu.2017.06.006. PubMed PMID: 28668578.

[14] M.M. de Rijk, A. Wolf-Johnston, A.F. Kullmann, S. Taiclet, A.J. Kanai, S. Shiva, et al., Aging-associated changes in oxidative stress negatively impacts the urinary bladder urothelium, Int Neurourol J. 26 (2) (2022) 111–118, https://doi.org/10.5213/inj.2142224.112. PubMed PMID: 35793989; PubMed Central PMCID: PMC9260322.

[15] Y.H. Lin, B.J. Chiang, C.H. Liao, Mechanism of action of botulinum toxin A in treatment of functional urological disorders, Toxins 12 (2) (2020), https://doi.org/10.3390/toxins12020129. PubMed PMID: 32085522; PubMed Central PMCID: PMC7077222.

[16] Y.H. Jiang, J.F. Jhang, H.C. Kuo, The clinical application of intravesical botulinum toxin A injection in patients with overactive bladder and interstitial cystitis, Tzu Chi Med. J. 35 (1) (2023) 31–37, https://doi.org/10.4103/tcmj.tcmj_313_21. PubMed PMID: 36866354; PubMed Central PMCID: PMC9972932.

[17] F. Weckx, M. Tutolo, D. De Ridder, F. Van der Aa, The role of botulinum toxin A in treating neurogenic bladder, Transl. Androl. Urol. 5 (1) (2016) 63–71, https://doi.org/10.3978/j.issn.2223-4683.2016.01.10. PubMed PMID: 26904413; PubMed Central PMCID: PMC4739988.

[18] A. Giannantoni, E. Costantini, S.M. Di Stasi, M.C. Tascini, V. Bini, M. Porena, Botulinum A toxin intravesical injections in the treatment of painful bladder syndrome: a pilot study, Eur. Urol. 49 (4) (2006) 704–709, https://doi.org/10.1016/j.eururo.2005.12.002. PubMed PMID: 16417964.

[19] R. Pinto, T. Lopes, B. Frias, A. Silva, J.A. Silva, C.M. Silva, et al., Trigonal injection of botulinum toxin A in patients with refractory bladder pain syndrome/interstitial cystitis, Eur. Urol. 58 (3) (2010) 360–365, https://doi.org/10.1016/j.eururo.2010.02.031. PubMed PMID: 20227820.